Journal of the Iranian Chemical Society
https://doi.org/10.1007/s13738-020-02024-8

ORIGINAL PAPER

Copper Schiff base complex as a new immobilized heterogeneous catalyst: experimental, theoretical, biological and docking study

Elham Zarenezhad[1] · Sheida Esmaielzadeh[2] · Somayeh Behrouz[3] · Leila Emami[4]

Received: 2 May 2020 / Accepted: 29 July 2020

Abstract

The novel copper$^{(II)}$ Schiff base complex was synthesized. Density functional theory calculations at the B3LYP (6-311G**/LANL2DZ) level of theory have been carried out to investigate the structure and geometry of the Schiff base ligand and its copper complex. IR spectra data (experimental and theoretical) show that the ligand Schiff base is coordinated to the copper ion in a bi-negative tetradentate manner with NNOS donor sites. From the theoretical data, it was found that the geometrical structure of this complex is distorted square planar. In continue, a safe, efficient, and improved procedure for synthesis of 1, 2, 3-triazole derivatives by immobilized [CuL] on silica is described. Terminal alkynes reacted with organic azides in the presence of a novel copper$^{(I)}$ catalyst, which is prepared by in situ reduction of the copper$^{(II)}$ Schiff base complex with ascorbic acid, in H_2O/THF at room temperature. Moreover, immobilized [CuL] on silica was approved to be a chemically and thermally stable catalyst that can be reused for several times with no significant loss in catalytic activity. The in vitro antifungal activities of title compounds were studied against *Candida albicans* (*ATCC 10231*), *Candida krusei* (*ATCC 6258*) and *Aspergillus niger* (*ATCC 16404*). Two compounds containing 2-(4-((((diphenylmethylene)amino)oxy)methyl)-1H-1,2,3-triazol-1-yl)-1-phenylethan-1-one and 2-(4-((((9H-fluoren-9-ylidene)amino)oxy)-methyl)-1H-1,2,3-triazol-1-yl)-1-phenylethan-1-one proved to have potent antifungal activity against *Candida albicans* and *Candida krusei.* A molecular docking study is also discussed for all synthesized compounds. The docking study demonstrated a significant interaction between the two most potent compounds and the active site of *Mycobacterium* P450DM.

Graphic abstract

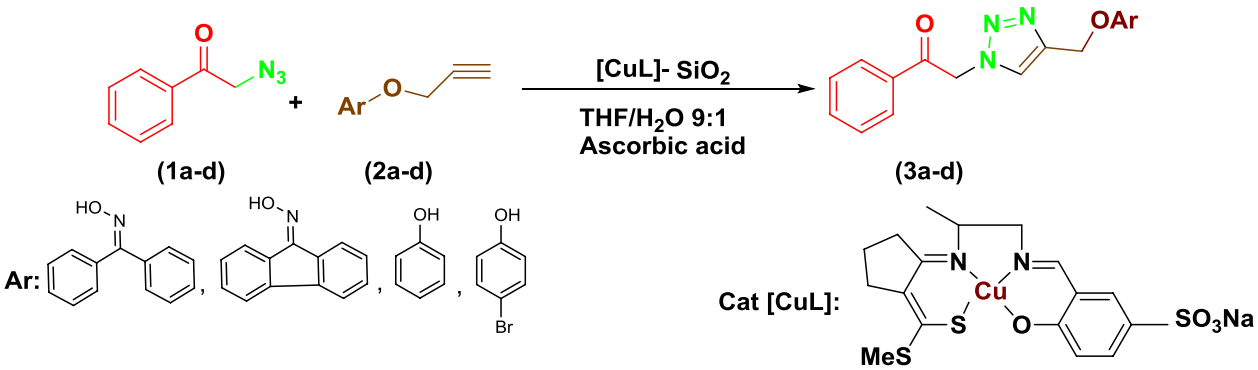

Keywords Click reaction · Copper Schiff base complex catalyst · Antifungal activities · Molecular docking analysis

Introduction

Heterocyclic compounds containing 1,2,3-triazole structure have a wide range of applications in biological systems [1]. Among them, 1,2,3-triazole frameworks are potential targets

✉ Sheida Esmaielzadeh
esmaielzadehsheida@gmail.com

Extended author information available on the last page of the article

Published online: 12 August 2020

for drug discovery because of their wide range of biological activities, such as antiviral, anticancer, anti-HIV, antibiotic, antibacterial, and antimicrobial [2]. 1, 2, 3 Triazoles are synthesized by azide-alkyne Click reaction which proposed for the first time by Rolf Huisgen in early 1960s, in which a mixture of 1, 4- and 1, 5-disubstituted 1,2,3- triazoles was formed [3]. Sharpless and Meldal [4, 5] have developed regioselective synthesis of 1,4-regio isomer in the presence of $Cu^{(I)}$ catalyst at room temperature, and this reaction became popular as Click reaction.

Catalysis (homogeneous and heterogeneous) plays a major impact on the chemical industry [6]. The development of heterogeneous catalysts for the synthesis of organic compounds has become a major area of research [7, 8]. Many Schiff base metal complexes display brilliant catalytic activity in various reactions such as Click reaction [9, 10], oxidation of organic compounds, polymerization reaction, hydroxylation, aldol condensation, hydrosilylation, epoxidation, reduction of ketones, and Henry reaction in the presence of moisture. Many Schiff base copper complexes have wide range of applications such as antiproliferative, anti-inflammatory, antiviral, and antimicrobial, properties. They were useful alternative for preparing various metal catalysts with different applications [11].

To improve the recovery and reuse, metal catalyst has been immobilized onto various supports such as silica gel [9], activated carbon [12], zeolites [13], amine-functionalized polymers [14], amine-functionalized silica [15], and aluminum oxyhydroxide fiber [16]. Also, immobilization of organometallic complexes on inorganic supports improved their stability, selectivity and the control of their reactivity of catalyst [17].

There are several procedures to support a homogeneous catalyst [18]. One of the most common methods is, to immobilize them on an insoluble supporting agent to achieve at so-called heterogenized homogeneous catalyst. The supports that are used in this approach include inorganic materials such as silica and organic polymers or alumina [19]. Inorganic supports such as silica gels are relatively cheap and can be used in most organic solvents; also supported catalysts based on silica gel can be separated from reaction media by means of simple filtration techniques [20]. Various copper$^{(I)}$ sources were used as catalyst such as CuI and CuOTf. $Cu^{(I)}$ can be in situ produced by using $CuSO_4{\cdot}5H_2O$ and sodium ascorbate as a reducing agent [21].

Recently, we immobilized homogeneous copper$^{(II)}$ catalyst on solid support which has been employed as reusable catalysts for regioselective 1,3-dipolar Huisgen cycloaddition [9]. In this context and in line with our interest in design and synthesis of new N-heterocycle derivatives [22–25], we report a new immobilized homogeneous catalyst system on silica based on Cu [26] and ascorbic acid as reducing agent for regioselective 1,3-dipolar Huisgen cycloaddition reaction to access 1,2,3-triazole cores (see Scheme 1).

Experimental

Materials and methods

General remarks

Melting points were determined with an Electrothermal 9100 apparatus. Elemental analyses were performed using a Heraeus CHN-O-Rapid analyzer. All preliminary chemicals were purchased from either Fluka or Merck. Solvents were purified by standard procedures. Reactions were followed by TLC using SILG/UV 254 silica-gel plates. Column chromatography was performed on silica gel 60 (0.063–0.200 mm, 70–230 mesh; ASTM). IR Spectra were obtained using a Shimadzu FT-IR-8300 spectrophotometer. NMR spectra were recorded on a Bruker Advance DPX-250 (^{1}H NMR at 250 and 400 MHz and ^{13}C NMR at 62.9 and 100 MHz) spectrometer in pure deuterated solvents with tetramethylsilane as an internal standard. GC/MS were performed on a Shimadzu GC/MS-QP 1000-EX apparatus (m/z; rel. %). The

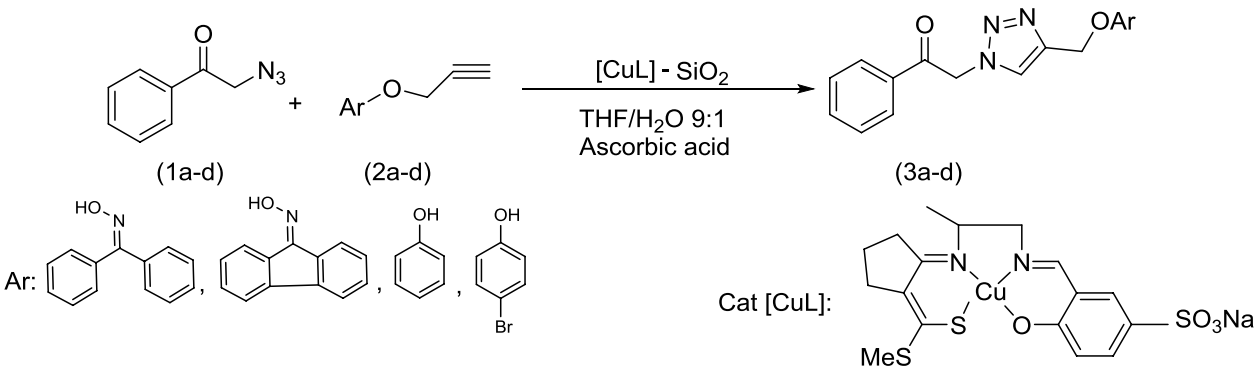

Scheme 1 Synthetic route of Huisgen cycloaddition reaction by the new CuII complexes catalyst

electronic absorption spectra were measured on PerkinElmer (LAMBDA 2) double beam. The magnetic susceptibilities of the copper complexes were carried out on Sherwood scientific magnetic susceptibility balance calibrated with $HgCO(NCS)_4$. Diamagnetic corrections were calculated from Pascal's constants. Molar conductance values (1×10^{-3} M) in DMF solution were determined by means of a Jenway 4310 conductivity meter and a diptype cell with a platinized electrode at room temperature.

Synthesis of the H_2L Schiff base ligand

The Schiff base ligand (H_2L) was prepared according to the procedure described in previously published method [22, 27]. The purity of the ligand was evaluated by thin layer chromatography.

Preparation of copper (II) complex

(0.23gr, 1 mmol) of H_2L Schiff base ligand was dissolved in 10 mL methanol/chloroform (1:2, V/V) and (0.19 g, 1 mmol) of $Cu(CH_3COO)_2$. H_2O in 10 mL ethanol was added to it. The resulting mixture was stirred for 24 h. The completion of the reaction was monitored by using TLC tests. TLC was performed on silica gel (Merck TLC plate) using appropriate solvent mixture (EtOAc/*n*-hexan) as eluent. The brown precipitate that formed was filtered off, washed several times with H_2O to remove unreacted metal ion and dried in air at room temperature. In spite of all the attempts, preparing of single crystal of copper (II) complex was unsuccessful.

Procedure for immobilization of [CuL] on silica

To a solution of [CuL] (0.5 g, 1 mmol) in anhydrous dichloromethane (50 mL), it was added a fresh and active silica gel (0.6 g, 10 mmol) in 0.063–0.200 mm or 70–230 mesh size. The suspension solution was stirred for 48 h at room temperature. Afterward, the suspension solution was flash filtered (sintered glass) and the solid residue (catalyst) was washed with anhydrous dichloromethane (2×50 mL). The catalyst was then dried in a vacuum oven at 60 °C for 4 h and stored in a refrigerator. Inductively coupled plasma (ICP) analysis indicated that in each gram of catalyst, there are 0.04 g of active Cu catalyst (0.05 mol%).

General procedure for catalytic test

To a round-bottom flask (50 mL) was added a mixture of alkyne (0.012 mol), catalyst (0.4 g, 0.05 mol%), the appropriate azide derivative (0.01 mol), and ascorbic acid (0.1 mol%) in a mixture of THF/H_2O (9:1, V/V, 20 mL). The reaction mixture was stirred at room temperature until TLC monitoring indicated no further progress in the conversion. The catalyst was filtered off, washed with THF/H_2O (5×10 mL), and the filtrate was evaporated under vacuum to remove the solvent. The remaining foam was dissolved in $CHCl_3$ (100 mL) and subsequently washed with water (2×100 mL). The organic layer was dried (Na_2SO_4) and evaporated. The crude product was purified by column chromatography on silica gel and eluted with proper solvents. Characterization data of all synthesized compounds are described below.

Spectra data for ligand

Methyl-2-{[3-(2-hydroxy-5-sodiumsulfitephenyl)methylidynenitrilo]propyl}amino-1-cyclopent-enedithiocarboxylate [H_2L](5) afforded the product as a yellow solid, yield: 65%; m.p.: 207 °C; IR (KBr, cm^{-1}): 766 (ν_{C-S}), 1152 ($\nu_{C-S+}\nu_{C-N}$), 1263 (ν_{C-O}), 1460 ($\nu_{C=C}$ aromatic), 1631 ($\nu_{C=N}$), 680, 1197 (ν_{S-O}, $_{S=O}$ stretching), 2960 (ν_{C-H}); 3379 (ν_{O-H}); ^{1}H NMR (δ, ppm, 250 MHz, DMSO-d_6): 1.26 (3H, d, $J=6.3$, Me), 1.75 (2H, m, $H^{4'}$), 2.39 (3H, s, SCH_3), 2.61 (2H, t, $J=4.1$, $H^{5'}$), 2.73 (2H, t, $J=4.1$ $H^{3'}$), 3.47–3.62 (3H, m, H^{en}), 6.77 (1H, d, $J=5.2$, H^3), 7.50 (1H, d, $J=5.2$, H^4), 7.66 (1H, s, H^6) 8.62 (1H, s, CH=N), 12.21 (1H, br, NH) and 13.12 (1H, br, OH); UV–Vis: λ_{max}(DMF, nm): 31 4, 396; MS Spectra: m/z(%) = 437$[M+1]^+$, 436$[M]^+$, 256, 236, 208, 185, 167, 111, 83, 57; ES-MS *m/z*; Found (Calc): $C_{17}H_{21}N_2O_4S_3Na$, C: 46.48 (46.77); H: 5.06 (4.85); N: 6.68 (6.42); S: 21.79 (22.03%).

Spectra data for Copper$^{(II)}$ Complex

{Methyl-2-[3-(5-sodiumsulfite-2-phenolate)methylidynenitrilo]propyl}aminato(-1)-1-cyclopent-enedithiocarboxylate copper (II) [CuL](6) afforded the product as a brown solid, yield (76%), m.dec. > 250 °C; IR (KBr, cm^{-1}): 738 (ν_{C-S}), 1110 ($\nu_{C-S+}\nu_{C-N}$), 1254 (ν_{C-O}), 1441 (benzene stretch), 1613, 1622 ($\nu_{C=N}$), 678, 1202 (ν_{S-O}, $_{S=O}$ stretching), 2943 (ν_{C-H}), 590(ν_{Cu-O}), 438(ν_{Cu-N}); UV–Vis: λ_{max}(DMF, nm): 328, 370, 396$^{(sh)}$; Λ_M = (10^{-3}M, in DMF, ohm^{-1} cm^2 mol^{-1}): 8.31; μ_{eff}: 1.79; MS Spectra: m/z (%) = 499$[M+1]^+$, 498$[M]^+$, 427, 393, 346, 328, 195, 172, 94, 73, 56; ES-MS *m/z*; Found (Calc): $C_{17}H_{19}N_2O_4S_3NaCu$, C: 41.20 (41.00); H: 4.08 (3.84); N: 5.36 (5.62); S: 19.57 (19.31%).

2-(4-((((Diphenylmethylene)amino)oxy)methyl)-1H-1,2,3-triazol-1-yl)-1-phenylethanone (3a) Column chromatography on silica gel (EtOAc/*n*-hexane = 2:1) afforded the product as a yellow solid, yield (92%), m.p 182–184 °C; R_f (EtOAc/n-hexane = 2:1, 0.64); IR (KBr, cm^{-1}): 3144, 2922, 1687, 1592, 1462, 1228 cm^{-1}; ^{1}H NMR (δ, ppm, 400 MHz, $CDCl_3$): δ: 5.52 (s, 2H, CH_2–N), 5.75(s, 2H, CH_2–O) 7.17–8.19 (m, 12H, arom, H-triazole), 8.16–8.19 (m, 4H, arom); ^{13}C NMR (δ, ppm, 100 MHz, $CDCl_3$): δ 54.4, 68.02, 118.74,

120.70, 124.14, 127.08, 127.26, 128.11, 128.51, 128.96, 130.04, 132.85,133.54, 134.35, 139.29, 140.32, 151.86, 189.18; ES-MS m/z = 396 [M + H]. Elemental Anal; Found (Calc): $C_{24}H_{20}N_4O_2$, C: 72.71(73.09); H: 5.08(4. 98); N: 14.13(13.98); O: 8.07 (8.09).

2-(4-((((9H-fluoren-9-ylidene)amino)oxy)methyl)-1H-1,2,3-triazol-1-yl)-1-phenylethanone (3b) Column chromatography on silica gel (EtOAc/*n*-hexane = 2:1) afforded the product as a yellow solid, yield (90%) m.p 190–193 °C; R_f (EtOAc/*n*-hexane = 2:1, 0.63); IR (KBr, cm^{-1}),: 3150, 2965, 1708, 1535, 1449, 1224 cm^{-1};^{1}H NMR (δ, ppm, 400 MHz, $CDCl_3$): δ: 5.30 (s, 2H,CH_2–N), 5.78(s, 2H, CH_2–O) 7.18–7.92 (m, 14 H, arom, H-triazole; ^{13}C NMR (δ, ppm, 100 MHz, $CDCl_3$): δ: 54.36, 66.54, 115.23, 123.98, 126.36, 127.12, 127.54, 128.16, 132.91, 133.60, 133.84, 134.10, 144.11, 153.33, 160.25, 189.22. ES-MS *m/z* = 394 [M + H]. Elemental Anal; Found (Calc): $C_{24}H_{18}N_4O_2$, C: 73.08 (72.96); H: 4.60 (4.80); N: 14.20 (14.44); O: 8.11(7.92).

2-(4-(Phenoxymethyl)-1H-1,2,3-triazol-1-yl)-1- phenylethanone (3c) Column chromatography on silica gel (EtOAc/*n*-hexane = 2:1) afforded the product as a yellow product; yield: (87%), m.p. 180–182 °FC; R_f (EtOAc/n-hexane = 2:1, 0.61); ^{1}IR (KBr, cm^{-1}): 3059, 2924, 1695, 1669, 1489, 1220. ^{1}H NMR (δ, ppm, 400 MHz, $CDCl_3$): 5.15 (2H, s, CH_2–N), 5.80 (2H, s, CH_2–O), 6.80–7.93 (11H, m, arom, H-triazole). ^{13}C NMR (δ, ppm, 100 MHz, $CDCl_3$): 54.4, 61.1, 112.4, 115.6, 124.9, 127.1, 128.2, 131.3, 132.8, 133.7, 156.3, 168.4, 189.0. ES-MS *m/z* = 394 [M + H]. Elemental Anal; Found (Calc): $C_{24}H_{18}N_4O_2$, C: 73.08 (73.16); H: 4.60 (4.69); N: 14.20(14.42); O: 8.11(7.92).

1-(4-Bromophenyl)-2-(4-(phenoxymethyl)-1H-1, 2,3-triazol-1-yl)ethanone (3d) Column chromatography on silica gel (EtOAc/*n*-hexane = 2:1) afforded the product as a yellow product; yield(80%), m.p 195–197 °C; R_f (EtOAc/*n*-hexane = 2:1, 0.59); IR (KBr, cm^{-1}): 3069, 2860, 1725, 1341 (C=N), 1466, 1263. ^{1}H NMR (δ, ppm, 400 MHz, $CDCl_3$): 5.15 (2H, s, CH_2–N), 5.80 (2H, s, CH_2–O), 6.71–8.03 (10H, m, arom, H-triazole). ^{13}C NMR (δ, ppm, 100 MHz, $CDCl_3$): 115.6, 127.1, 127.7, 128.2, 129.8, 131.3, 132.8, 133.7, 156.2, 166.7, 189.0. Elemental Anal.: Found (Calc): $C_{17}H_{14}N_3O_2Br$, C: 54.80 (54.86); H: 3.83 (3.09); N: 11.25 (11.89).

Results and discussion

Initially, we prepared an active catalyst, as is shown in Scheme 2. Firstly, the unsymmetrical Schiff base ligand (**5**) was prepared by condensation of the methyl 2-((1-aminopropan-2-yl)amino)cyclopent-1-ene-1-carbodithioate (**4**) and 5-sodiumsulfitesalicyl aldehyde in methanol. Compound (**4**) was synthesized by published methods [27]. Then, the resultant yellow powder was recrystallized from methanol/chloroform 2:1(V/V). The $Cu^{(II)}$ complex (**6**) was obtained from addition of (1 mmol) of the appropriate Schiff base ligand (yellow color) in 10 mL of chloroform/methanol 2:1 (V:V), into a solution of 1 mmol of copper acetate in 10 mL of ethanol. The solution was stirred for 15 min and then allowed to stand at room temperature for 24 h. After filtering, the brown precipitate was washed several times with H_2O and ethanol and finally filtered and dried in air at room temperature. In spite of all the efforts, the copper$^{(II)}$ complex could not be crystallized.

Theoretical calculation studies of copper$^{(II)}$ complex

By increasing development of theoretical chemistry, DFT has been extensively used due to their accuracy and low

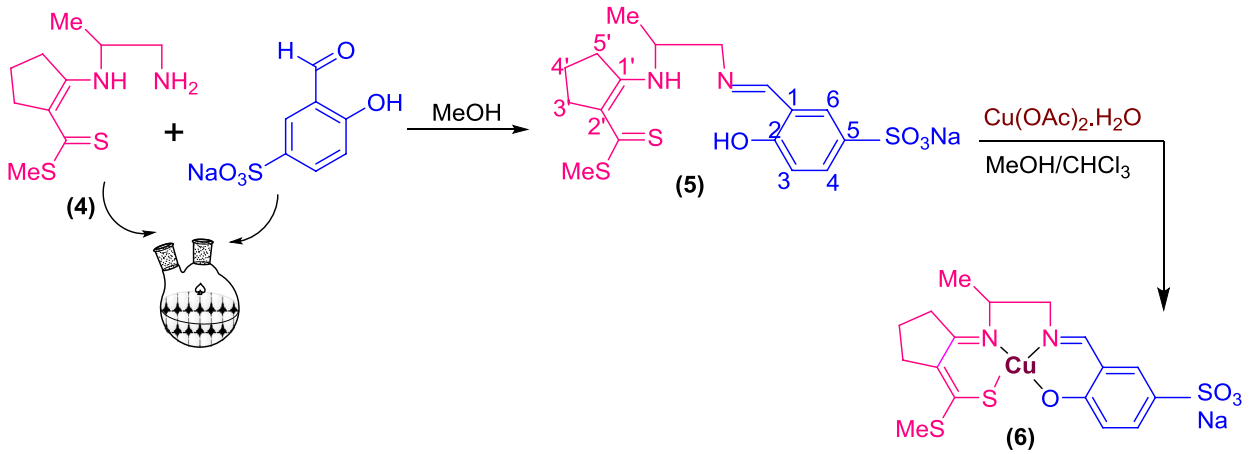

Scheme 2 Synthesis of Copper$^{(II)}$ Complex

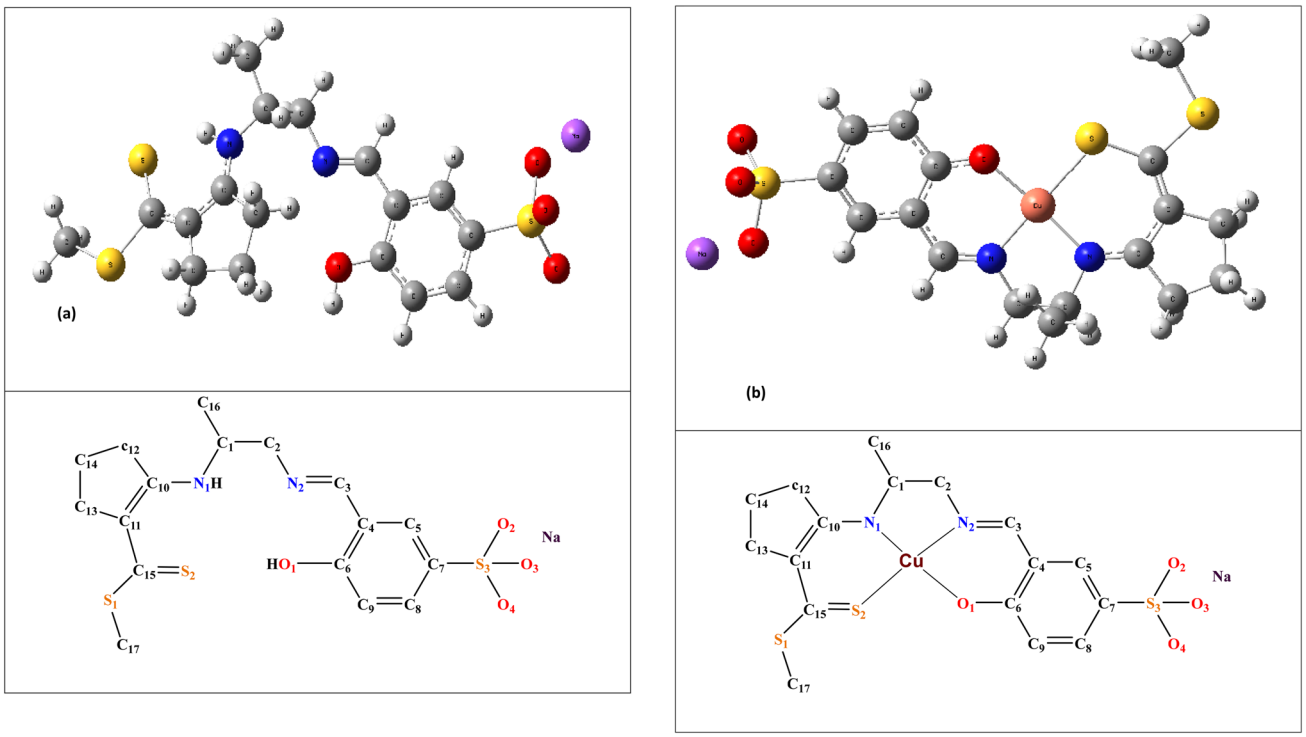

Fig. 1 Geometry optimized structure of **a** Schiff base ligand, **b** Cu (II) complex

computational cost to calculate a wide variety of molecular properties to access reliable results which are in accordance with experimental values. In present work, the geometry optimization of the Schiff base ligand and its copper complex were performed with the nonlocal gradient corrected B3LYP density functional with standard 6-311G** basis set [28] for all elements except Cu and LANL2DZ [29] with effective core potential for Cu atom, using the Gaussian 03 software package [30].

After optimization the vibrational frequency analyses were calculated at the same level of theory, with the keyword freq and pop indicating that the optimized structures are at the stationary points corresponding to local minimal without any imaginary frequency. The gas phase optimized structure of H_2L and [CuL] along with labeling atoms is shown in Fig. 1. The optimized parameters (bond lengths, bond angles) and some electronic properties such as HOMO and LUMO energies, chemical hardness and IR data of the titled compounds were obtained by using the B3LYP/6-311G**- LAN2DZ method and were discussed in details (see Tables 1, 2).

The H_2L ligand molecule deprotonates and then acts as a tetradentate dianionic Schiff base ligand framework. It can be easily seen that the ligand is not planar since the theoretical dihedral angles between the phenyl ring and cyclopentene ring on the right side of the ligand molecule. The calculated (N1–C1)(1.445 Å), (N1–C10)(1.448 Å) and (N2–C2)

Table 1 Selected calculated structural parameters of the Schiff base ligand and Cu(II) complex

	Band length (Å)		Bond angle (°)	
	H2L	CuL	CuL	
N1–C1	1.445	1.443	N1–Cu–N2	87.407
N1–C10	1.448	1.320	N1–Cu–O1	175.151
N2–C2	1.447	1.440	N1–Cu–S2	90.716
N2–C3	1.306	1.316	N2–Cu–O1	91.148
O1–C6	1.383	1.394	N2–Cu–S2	174.143
S2–C15	1.648	1.663	O1–Cu–S2	86.217
Cu–N1	–	1.947		
Cu–N2	–	1.949		
Cu–O2	–	1.912		
Cu–S2	–	2.127		

Table 2 Calculated quantum chemical descriptors at B3LYP method with mix basis set

Complexes	HOMO/eV	LUMO/eV	Gap/eV	Hardness(η)
H2L1	− 5.453	− 3.331	2.099	1.049
[CuL(SO3Na)]	− 5.297	− 1.702	3.595	1.797
[CuL(NO2)] [2]	− 5.281	− 1.633	3.648	1.824

(1.447 Å) bond lengths are of the approximate value for a C–N single bond length, whereas the (N2–C3) (1.306 Å) has a double bond character which is comparable to the other C–N single bond values in this molecule. The calculated (O1–C6) (1.383 Å) and (S2–C15)(1.648 Å) bond distances are somewhat between the length of a C–O (1.43 Å) [26] and C–S (1.82 Å) [31] single bond that of a C=O (1.20 Å) [26] and C=S (1.55 Å) [31] double bond. These values suggest that electron density may be delocalized throughout the N2–C4–C5 fragment, the aromatic ring and the O1–C10 bond on the right side and N1–C10–C11, cyclopentene ring and C15–S2 bond on the left side of this ligand. The Schiff base ligand is coordinated to the copper metal core through the phenolic oxygen atom (O1), the amine nitrogen (N1), azomethine nitrogen atom (N2) and thio sulfur atom (S2). The Cu–N1, Cu–N2, Cu–O1 and Cu–S2 bond distance in [CuL] is 1.947 Å, 1.949 Å, 1.912 Å and 2.127 Å, respectively.

Theoretical bond lengths and bond angles for the [CuL] complex show the copper atom is slightly distorted from the square planar geometry. For example the calculated angles obtained for N1–Cu–O1 and N2–Cu–S2 are 175.151° and 174.143°, respectively, instead of 180°.

The agreement between the bond distances and bond angles results obtained by experimental similar compounds and theoretical studies is reasonably good [27]. It should be noted that some observed differences are most probably to the X-ray crystal diffraction being applied in the solid phase, while theoretical calculations were carried out in the gas phase [22].

IR spectra have proven to be the most suitable technique to give enough information to elucidate the way of bonding of the ligand to the metal ion. In Table 3 we compared some important normal mode harmonic vibrational wavenumbers obtained from DFT calculations with those of the experimentally measured bands of the titled compounds. The broad and medium band assigned to O–H stretching vibration of the phenolic OH group appears at 3325 cm^{-1} in the [H_2L] Schiff base ligand spectrum. In the [CuL] complex the O–H peak disappears. This result indicates that complexation occurred and suggests that the phenolic oxygen atom is involved in the coordination sphere [32]. The IR multiple bands at around 2900 in the ligand and its copper complex are attributed to C-H stretching vibration. The stretching vibration of C=N observed at 1631 cm^{-1} of infrared spectra of Schiff base ligand shifted to lower frequency side 1613 and 1622 cm^{-1} in the spectra of the [CuL] complex indicate that involvement of azomethine N atom are coordinated to Cu(II) [33].

The sharp and other band which occurs at 1460 cm^{-1} and 1441 cm^{-1} in the free ligand and its Cu complex can be assigned to the aromatic C=C stretching vibration [34]. The IR spectrum of the free ligand contains strong C–O

Table 3 Comparison of some important IR vibrational modes (cm^{-1}) between experimental and theoretical computed of the [H_2L] Schiff base and [CuL] complex

	Compound	υ (Cu–N)	υ (Cu–Od)	υ(C=S)	υ(C–S + C–N)	υ(C–O)	υ(C=C)	υ(C=N)	υ(C–H)	υ(O–H)	υ(SO_3)
Experimental	H2L	–	–	766	1152	1263	1460	1631	2960	3325	680, 1197
	[CuL]	438	560	738	1110	1244	1441	1613, 1622	2943	–	678, 1199
Calculated frequencies	H2L	–	–	789	–	1260	1468	1651	3005	3391	683, 1202
	[CuL]	475	573	729	–	1279	1453	1627	2998	–	685, 1203

absorption band at 1263 cm^{-1}. This band appeared at 1254 cm^{-1} in the spectrum of the complex, indicating that the Schiff base ligand coordinates to the metal center through deprotonated form [35]. A medium to strong intensity band at 1152 and 766 cm^{-1} due to ν(CS + CN) and (CS) of the ligand shifted to lower wavenumber in the [CuL] complex which indicates the coordination of the thio sulfur atom [22]. Non-ligand band at 560 cm^{-1} and 438 cm^{-1} was assigned to ν(Cu–O) and ν(Cu–N), respectively [36]. The frequencies characteristics of S–O stretching modes in the IR spectra of the free ligand were observed around 680 and 1200, respectively. These absorption bands remained almost at the same position in the [CuL] complex, suggesting that SO_3 group is not involved in coordination [27]. These experimental values were also in good correlation with computational studies. Generally, the correlation suggests that the computed structures are reliable and give credence to conclusions arrived at from an analysis of the functional density theory. The small differences between the calculated and experimental vibrational wavenumber are likely to originated from (1) the environmental solvent conditions and (2) the experimental values are anharmonic frequencies while the calculated values are aromatic [31].

The frontier orbitals (HOMO and LUMO orbitals) are very important parameters in quantum chemistry. The difference energy levels between HOMO and LUMO orbitals [17] help us to characterize the chemical reactivity and kinetic stability of the molecule. An electronic system with a larger Eg should be less reactive than having smaller gap [15, 37]. The HOMO and LUMO energies [17] and contour diagram of these FMOs (frontier molecular orbitals) of mentioned ligand and its Cu complex are represented in Table 2 and Fig. 2. According to Fig. 2, the HOMO electron density distribution for the Schiff base ligand is located over all cyclopentene ring and N1 atom, and the LUMO level of the charge density is mostly dominated for benzene ring, N2 and O1 atoms, while the complex HOMO electron orbitals are mainly localized on bridging nitrogen atoms, O1 and sulfur atoms (S1, S2) in ligand and Cu metal atom. The LUMO includes contributions from both, Cu central atom and other interacting ligand hetero atoms.

The energy gaps ($Eg = E_{LUMO} - E_{HOMO}$) are found to be 2.099 and 3.595 eV, for the H_2L and [CuL] compounds, respectively. The Eg in H_2L is smaller than the [CuL]. As the Eg decreases the reactivity is increased; so, the free ligand is more polarized, less stable and more reactive molecule, i.e., the electronic charge transfer from the ligand (easily offer electrons to an acceptor) to the central metal ion increase.

Other important parameter in quantum chemistry is hardness because the chemical hardness is useful to rationalize the relative stability and reactivity of chemical compound. The hardness corresponds to the HOMO and LUMO gap energy ($\eta = 1/2Eg$) [38]. On the basis of the data in Table 2 the [CuL] complex with large hardness and less Eg has more stability and less chemical reactivity than the ligand and it is hard molecule.

The comparison of the analysis of molecular orbitals for the [CuL] complex in this paper and [CuL^1] [21] shows that the Eg of [CuL^1] complex is larger than that of the [CuL] indicating the chemical reactivity of the [CuL^1] complex is decreased and the complex is more stable, so the trend of catalytic activity was found to be [CuL^1] < [CuL]. This results support the experimental catalytic properties for the Click reaction which was studied in this work.

Catalytic study

After synthesis and supporting the catalyst on silica gel, we used this catalyst for the synthesis of some 1,2,3-triazole derivatives. Initially, to obtain the optimized reaction conditions, we selected the reaction of 2-azido-1-phenylethanone with benzophenone O-prop-2-yn-1-yl oxime as a model reaction to produce the corresponding 1,2,3-triazole (**3a**) (Table 4). This reaction carried out in the presence of ascorbic acid (0.1 mol%) and [CuL]–SiO_2 (0.05 mol%) in various 2:1 (V/V) organic solvents/H_2O at room temperature (Table 4). As can be seen in Table 4, it is well demonstrated the solvent has a significant role in progress of reaction.

The most appropriate result was obtained when a THF/H_2O mixture was applied (Table 1, entry 5). However, other mixtures also afforded moderate to good yields of **3a** after longer times (Table 4, entries 1–4, and 6). When H_2O was used alone, the low yield of **3a** was attained after 4 h which is attributed to the lack of solubility of the starting materials in H_2O under the examined condition (Table 4, entry 7). Also, the low yield of **3a** was obtained using pure THF after 4 h (Table 4, entry 8).

To investigate the optimized amount of [CuL]–SiO_2, different amounts of catalyst were examined in the model reaction (Table 5). As shown in Table 5, the best result was obtained when 0.05 mol% catalyst was used (Table 5, entry 5). The use of an excess amount of the catalyst has no considerable effect on the progress of the reaction (Table 5, entries 6 and 7).

To determine the catalytic potency of [CuL]–SiO_2 in the synthesis of **3a**, we tested the model reaction using other Cu catalysts and compared the results with that of [CuL]–SiO_2 (Table 6).

When the reaction was accomplished in the absence of catalyst, no product was obtained even if the reaction time was prolonged (Table 6, entry 1). As depicted in Table 6, shorter reaction time and higher yield of **3a** were obtained using homogeneous and heterogeneous [CuL] (Table 6, entries 2 and 3) in comparison with other examined copper catalysts. Previously, we synthesized two new complex of $cu^{(II)}$ as an effective catalyst. In this study, we compared the

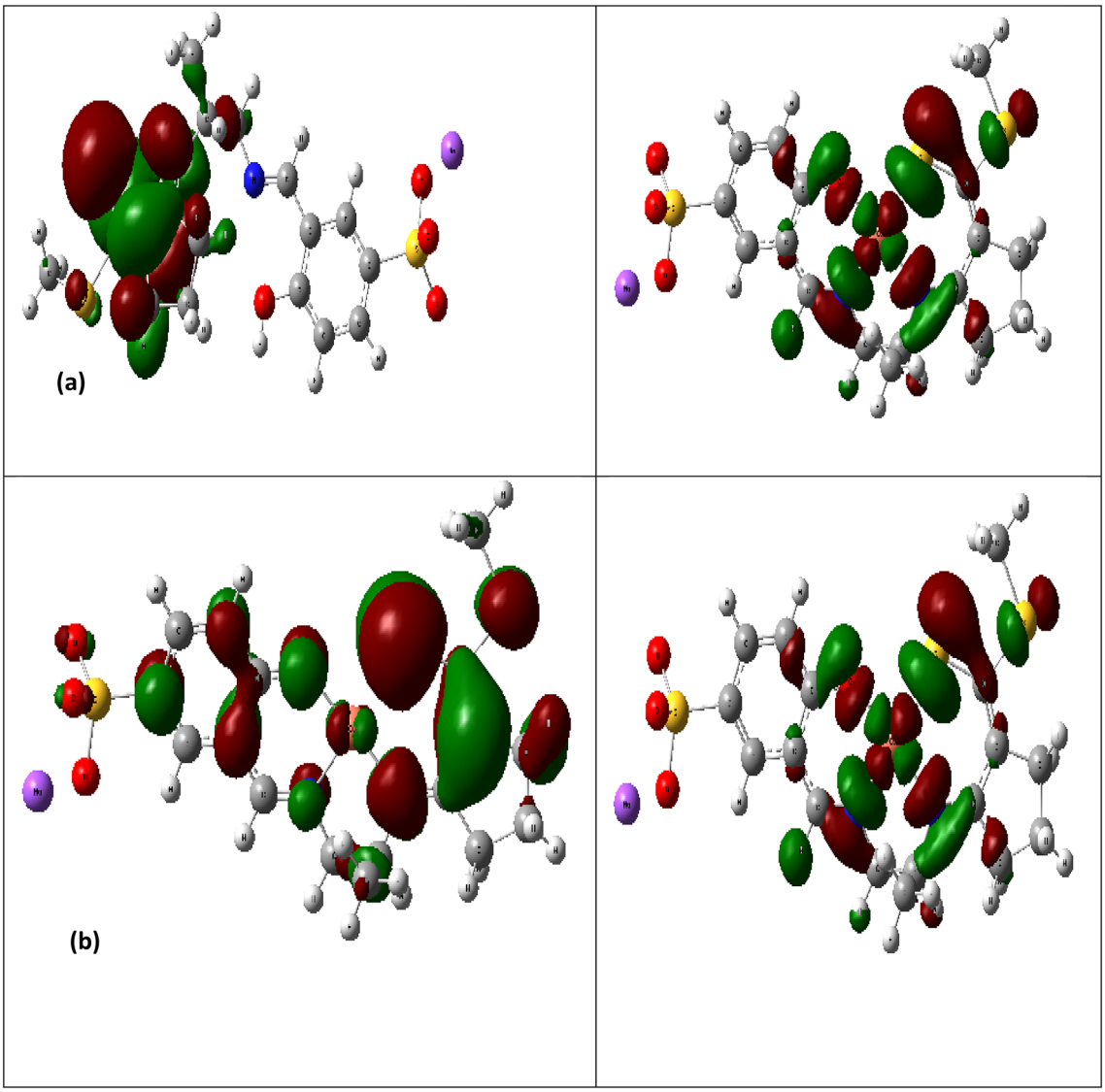

Fig. 2 The plot of HOMO (left) and LUMO (right) calculated molecular orbital levels of **a** H_2L and **b** [CuL]

catalytic effect of new copper complex [CuL] in this study with [CuL2] and [CuL2] complexes in Ref. [22] (Table 6, entries 4 and 5). The reaction yield obtained using new catalyst is higher than that of the previous catalysts. Also, the new catalyst required shorter reaction time in comparison with that of previous catalyst. NO_2 [22] and SO_3 substituents are both an electron withdrawing group. This group removed electron density from π-system making the Schiff base ligand more electrophilic. The acceptor property of the Schiff base ligand is increased by decreasing the electron donating properties of the NO_2 and SO_3 groups; the trend of the acceptation effect of the Schiff base ligand is as follow: $H_2L–SO_3 > H_2L–NO_2$ and therefore leads to decrease in the kinetic stability of the copper complex i.e., the following trend complex formation of a given Cu cation toward the Schiff base ligand is: ($[CuL–NO_2] > [CuL–SO_3]$). So, the catalytic activity of the ($[CuL–NO_2]$ is less than the $[CuL–SO_3]$). According to the results in Table 6 (entries 2 and 3), both of heterogeneous and homogeneous [CuL] catalyst are effective, but we applied immobilized [CuL] on silica as a heterogeneous catalyst, because it has many advantages such as easy catalyst separation and recovery, regeneration, and reuse. To prevent the formation of by-products because of alkyne-alkyne homo-coupling reaction in the presence of $Cu^{(I)}$ salts, we optimized the stoichiometric ratio of azide/alkyne which was found to be 1:1.2 for synthesis of **3a** when 0.05 mol% of catalyst was applied.

To assess the scope of this method, we extended the optimized reaction condition to other alkynes and azide cycloadditions (Table 7). As the shown in Table 6, $[CuL]–SiO_2$

Table 4 Influence of various miscible organic solvents on conversion of benzophenone O-prop-2-yn-1-yl oxime into 3a using [CuL]–SiO_2 at room temperature

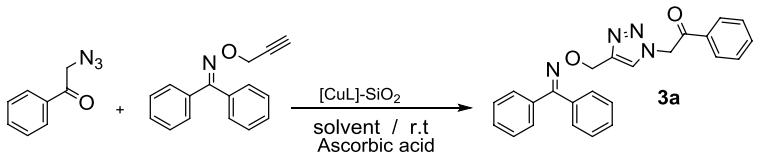

Entry	Solvent[a]	Time (h)	Yield[b] (%)
1	H_2O/DMSO	1.5	80
2	$H2_O$/DMF	1.5	79
3	H_2O/t-BuOH	1.5	70
4	H_2O/MeCN	1.5	60
5	H_2O/THF	1	92
6	H_2O/acetone	4	63
7	H_2O	4	39
8	THF	4	48

[a]For entries 1–7, a mixture of 1:2 (V/V) solvents were used

[b]Isolated yield

Table 5 Influence of different amounts of catalyst on conversion of benzophenone O-prop-2-yn-1-yl oxime into **3a** at room temperature

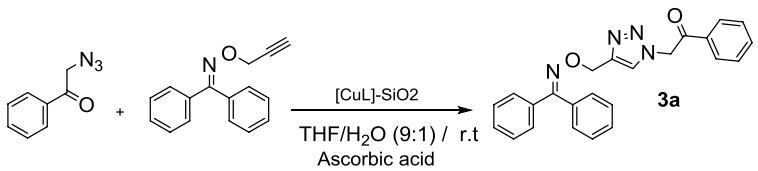

Entry	[CuL]–SiO_2 (mol%)	Time (h)	Yield[a] (%)
1	0.01	4	40
2	0.02	3	52
3	0.03	3	60
4	0.04	2	65
5	0.05	1	92
6	0.06	1	92
7	0.07	1	92

[a]Isolated yield

proved to be effective catalyst for Huisgen cycloaddition between different α-azido ketones and alkynes. The structures of all synthesized compounds **3a–3d** were characterized by IR, ^{1}H NMR and ^{13}C NMR, and elemental analyses.

Antifungal studies

The in vitro antifungal activity of 1,2,3-triazol molecules **3a–3d** was assessed against some pathogenic fungi comprising *Candida albicans* (*ATCC 10231*), *Candida krusei* (*ATCC 6258*) and *Aspergillus niger* (*ATCC 16404*). The minimal inhibitory concentrations (MICs) of the tested compounds were determined by the micro-broth dilution method in 96-well microplates according to the CLSI-M27-A3 [39]. The specified amount of triazole compounds was dissolved in DMSO and serially diluted in the standard RPMI-1640 medium (Sigma Chemical Co.) bicarbonate (maximum concentration was considered 512 µg/mL for all compounds). Briefly, the inoculum suspension was added to each well and incubated at 35 °C.

Table 6 Comparison of our previous copper catalysts with [CuL]–SiO_2 for preparation of **3a**

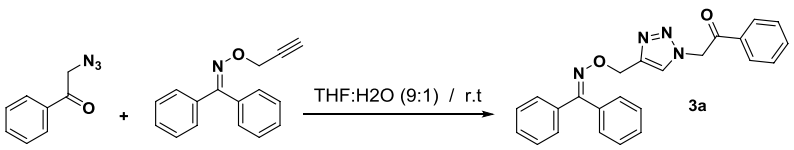

Entry ref	Catalyst	Time (h)	Yield[a] (%)
1	–	5	0
2	Hetero [b]	1	92
3	Homo [c]	1	92
4 [22]	[CuL1]	2	74
5 [22]	[CuL2]	2	88

[a]Isolated yield

[b]Heterogeneous [CuL]

[c]Homogeneous [CuL]

Table 7 'Click' cycloaddition of azides with alkynes

Entry	Bromo keton or alkyl halid (1)	Acetylens (2)	Product (3)	Time (min)	Yelid	Mp ^{O}C Lit, [ref]
1	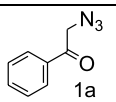	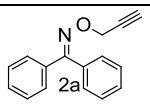	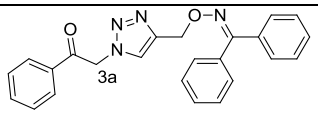	60	92	In this wok 182–184
2	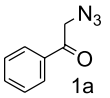	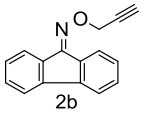	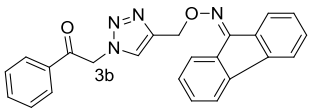	60	90	In this wok 190–193
3	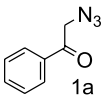	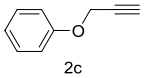	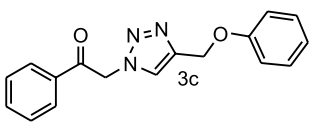	60	87	180–183 182[22]
4	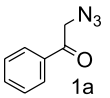	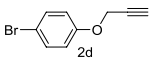	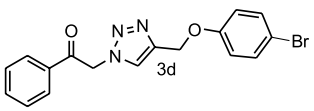	60	80	195–197 197[22]

All susceptibility testing was performed in duplicate. Fluconazole (FLZ) was chosen as the reference drug. As the MIC values indicate (Table 8), **3a** was the most potent agents against all tested fungal species; also **3b** showed antifungal activity.

Molecular docking studies

Molecular docking simulation of all synthesized compounds (**3a**–**3d** and fluconazole) was done to investigate the possible interaction and free binding energy (kcal.

Table 8 In vitro antifungal profiles of **3a–3d**

Compound	MIC[a] (μg/ml)		
	Candida albicans	*Candida krusei*	*Aspergillus niger*
3a	32	64	128
3b	64	64	128
3c	128	128	256
3d	256	128	128
Fluconazole[b]	0.25	64	2

Examined fungi: *Candida albicans* (*ATCC 10231*), *Candida krusei* (*ATCC 6258*) and *Aspergillus niger* (*ATCC 16404*)

[a]Minimal inhibitory concentration

[b]Reference drugs for fungal species

Table 9 The bonding energies (kcal mol^{-1}) of the tested compounds using AutoDock Vina

Compounds	Binding energy (Kcal mol^{-1}) for 1EA1	Log *P*
3a	− 11.9	4.91
3b	− 11.4	4.55
3c	− 9.8	2.93
3d	− 9.7	3.75
CO-crystal ligand	− 8.9 (fluconazole)	0.99

mol^{-1}) of ligand-complex into the active site of lanosterol 14α-demethylase enzyme (1EA1). All the docking protocols were done on validated structures, with RMSD values below 2 Å. The range of binding energy was seen between − 11.9 (Kcal mol^{-1}) to − 9.7 (Kcal mol^{-1}). Fluconazole binding energy was observed at − 8.9 (Kcal mol^{-1}) (Table 9).

All the tested compounds showed high docking binding energies than the co-crystal ligands (fluconazole), and the compounds **3a**, **3b** had the best binding energy values as well as highest antifungal activity. The good biological activity of compounds **3a, 3b** can be described to their strong binding affinity with lanosterol 14α-demethylase enzyme. This may be caused better hydrophobic and van der Walls interactions between diphenyl and fluorene moiety of **3a** and **3b** compounds with Fe^{2+} in the heme molecule of 14α-demethylase. On the other hand, it seems to be related to the ratio of their lipophilicity and electronegativity. It should be noted that suitable hydrophilicity/lipophilicity balance can enhance the penetration to fungal cells [40, 41]. As it is shown in Fig. 3, pi–pi bond interaction exists between 1, 2, 3 triazole group of **3a**, **3b** and Tyr 76. There is also existed a pi-hydrogen bond interaction between phenyl groups of diphenyl oxime of **3a** with Ala 256 at distance 3.99 Å. Compound **3c** has hydrogen bond interaction between 1,2, 3 triazole groups with Arg 96 at distance 3.27 Å. As depicted in Fig. 3, the carbonyl group between 1, 2, 3 triazole and phenyl ring is involved in hydrogen bond interaction with residue Ala 256 at distance 3.47 Å in compound 3d.

Docking study

The X-ray crystallographic structure of cytochrome P450 14α-demethylase (PDB ID: 1EA1) was obtained from Protein Data Bank (PDB data base; http://www.rcsb.org), and converted to PDBQT using the MGLTOOLS 1.5.6 [42]. The chemical structures of the tested compounds were drawn and optimized by the ChemBioDraw (version 12.0) and HyperChem Professional Version 8 (Hypercube Inc., Gainesville, FL, USA).

AutoDock Tools 1.5.4 program was used for all the preprocessing steps for receptor structure, and tested ligands were performed (8) (The Scripps Research Institute, La Jolla, California, USA) [43]. The co-crystal ligand was redocked, to verify the validation of docking calculations, and the final docked conformations resulted in 1–1.5 Å root-mean-square deviation. The Lamarckian genetic algorithm (LGA) was applied to model the interaction between ligands and 14α-demethylase active site. For the Lamarckian genetic algorithm: 27,000 maximum generations; a gene mutation rate of 0.02 and a crossover rate of 0.8 were applied. The grid box size was set to 40 × 40 × 40 points in *x*, *y* and *z* directions, respectively. The box was centered based on the co-crystal ligand with a spacing of 0.375 Å. Cluster analysis was performed on the docked results using an RMSD (root-mean-square deviation) tolerance of 2 Å. All interactions were visualized and evaluated on the basis of docking results by VMD software [44].

Conclusions

Synthesis and characterization of Schiff base ligand and its Cu^{II} complex were described. Then, the computational study allows us to obtain optimized structure, molecular parameters, HOMO, LUMO, and HOMO–LUMO band gap, IR vibrational frequencies, characteristics of new tetradentate copper complex. Immobilized [CuL] on silica as a new and convenient heterogeneous catalyst was demonstrated to be an efficient, thermally and chemically stable, environmental compatible and low-cost catalyst that can be easily prepared and reused for many consecutive runs without a significant decrease in its catalytic reactivity. The catalytic study has shown a simple, one-pot reaction between terminal alkynes and organic azides in the presence of [CuL]–SiO_2, which gave very good to excellent yields of medicinally important nitrogen heterocycles. The advantages of the reported method are short reaction time, simple method and high yields. The antifungal tests have shown antifungal activity

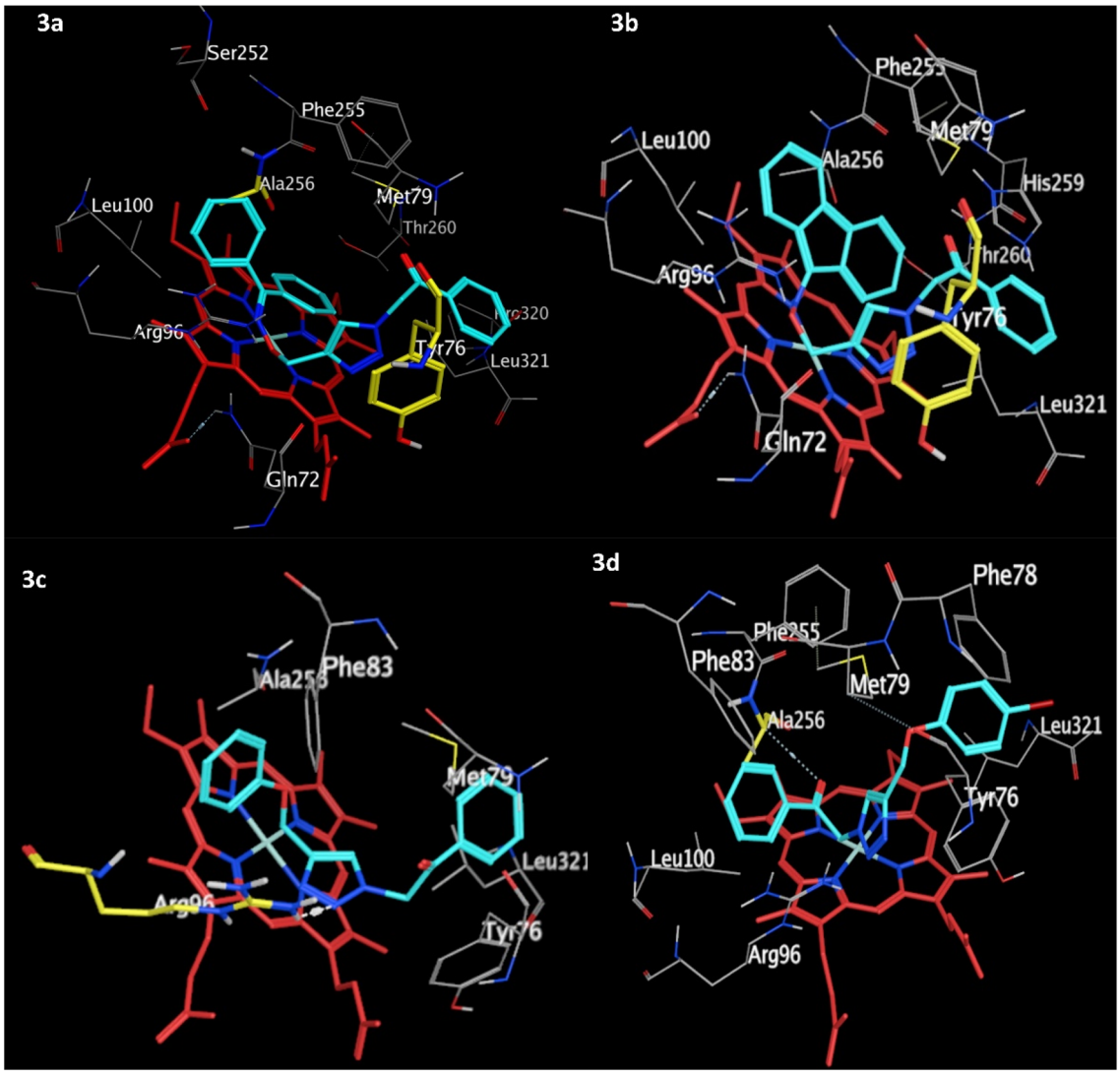

Fig. 3 Interactions of **3a**, **3b**, **3c** and **3d** with the residues in the binding site of 1EA1 receptor

against two tetrazole compounds. The docking analysis has demonstrated the appropriate fitting of **3a** and **3b** in active site of *Mycobacterium* P450DM enzyme.

Acknowledgements This study was supported by Fasa University of Medical Sciences and Islamic Azad University, Darab Branch.

Compliance with ethical standards

Conflict of interest The authors declare that they have no conflict of interest.

References

1. S. Behrouz, M.N.S. Rad, S. Rostami, M. Behrouz, E. Zarehnezhad, A. Zarehnezhad, Mol. Divers. **18**, 4 (2014)
2. D. Dheer, V. Singh, R. Shankar, Bioorg. Chem. **1**, 71 (2017)
3. R. Huisgen, Angew. Chem. Int. Ed. **2**, 10 (1963)
4. V.V. Rostovtsev, L.G. Green, V.V. Fokin, K.B. Sharpless, Angew. Chem. Int. Ed. **14**, 41 (2002)
5. C.W. Tornøe, C. Christensen, M. Meldal, J. Org. Chem. **67**, 9 (2002)
6. E. Farnetti, R. Di Monte, J. Kašpar, in *Inorganic and Bio-Inorganic Chemistry,* ed by I. Bertini, vol. 6, Eolss, Oxford (2009)
7. G. Sartori, R. Ballini, F. Bigi, G. Bosica, R. Maggi, P. Righi, Chem. Rev. **104**, 1 (2004)
8. H.G. Hosseini, E. Doustkhah, M.V. Kirillova, S. Rostamnia, G. Mahmoudi, A.M. Kirillo, Appl Catal. A Gen. **25**, 96 (2017)
9. E. Zarenezhad, M.N.S. Rad, S. Behrouz, S. Esmaielzadeh, M. Farjam, J. Iran. Chem. Soc. **14**, 2 (2017)
10. M.N. SoltaniRad, S. Behrouz, J. Mohammadtaghi-Nezhad, E. Zarenezhad, M. Agholi, Appl. Organomet. Chem. **33**, 4 (2019)
11. A.M. Abu-Dief, I.M. Mohamed, J. Basic Appl. Sci. **4**, 2 (2015)
12. B.H. Lipshutz, B.R. Taft, Angew. Chem. Int. Ed. **45**, 48 (2006)

13. S. Chassaing, M. Kumarraja, A. SaniSounaSido, P. Pale, J. Sommer, Org. Lett. **9**, 5 (2007)
14. C. Girard, E. Önen, M. Aufort, S. Beauvière, E. Samson, J. Herscovici, Org. Lett. **8**, 8 (2006)
15. T. Miao, L. Wang, Synthesis **03**, 2008 (2008)
16. M.S. Kwon, N. Kim, C.M. Park, J.S. Lee, K.Y. Kang, J. Park, Org. Lett. **7**, 6 (2005)
17. C. Baleizao, H. Garcia, Chem. Rev. **106**, 9 (2006)
18. V.S. Shende, V.B. Saptal, B.M. Bhanage, Chem. Rec. **19**, 9 (2019)
19. K. Mori, T. Hara, T. Mizugaki, K. Ebitani, K. Kaneda, J. Am. Chem. Soc. **125**, 38 (2003)
20. R.E. Patterson, *Preparation and Uses of Silica Gels and Precipitated Silicas* (ACS Publications, Wasington, DC, 1994), p. 618
21. L. Zhang, X. Chen, P. Xue, H.H. Sun, I.D. Williams, K.B. Sharpless, V.V. Fokin, G. Jia, J. Am. Chem. Soc. **127**, 46 (2005)
22. S. Esmaielzadeh, E. Zarenezhad, Acta Chim. Slov. **65**, 2 (2018)
23. M.H. Afsarian, M. Farjam, E. Zarenezhad, S. Behrouz, M.N.S. Rad, Acta Chim. Slov. **66**, 4 (2019)
24. M.N.S. Rad, S. Behrouz, M. Behrouz, A. Sami, M. Mardkhoshnood, A. Zarenezhad, E. Zarenezhad, Mol Divers. **20**, 3 (2016)
25. E. Zarenezhad, M.N.S. Rad, M.H. Mosslemin, M. Tabatabaee, S. Behrouz, J. Chem. Res. **38**, 10 (2014)
26. A. Akbari, Z. Alinia, Turk. J. Chem. **37**, 6 (2013)
27. M. Asadi, K. Mohammadi, S. Esmaielzadeh, B. Etemadi, H.K. Fun, Polyhedron **28**, 8 (2009)
28. A.D. Becke, J. Chem. Phys. **98**, 492 (1993)
29. C. Lee, W. Yang, R.G. Parr, Phys. Rev. B. **37**, 2 (1988)
30. M.J. Frisch, G.W. Trucks, H.B. Schlegel, G.E. Scuseria, M.A. Robb, J.R. Cheeseman, J.A. Montgomery, J.T. Vreven, K.N. Kudin, J.C. Burant, J.M. Millam, S.S. Iyengar, J. Tomasi, V. Barone, B. Mennucci, M. Cossi, G. Scalmani, N. Rega, G.A. Petersson, H. Nakatsuji, M. Hada, M. Ehara, K. Toyota, R. Fukuda, J. Hasegawa, M. Ishida, T. Nakajima, Y. Honda, O. Kitao, H. Nakai, M. Klene, X. Li, J.E. Knox, H.P. Hratchian, J.B. Cross, C. Adamo, J. Jaramillo, R. Gomperts, R.E. Stratmann, O. Yazyev, A.J. Austin, R. Cammi, C. Pomelli, J.W. Ochterski, P.Y. Ayala, K. Morokuma, G.A. Voth, P. Salvador, J.J. Dannenberg, V.G. Zakrzewski, S. Dapprich, A.D. Daniels, M.C. Strain, O. Farkas, D.K. Malick, A.D. Rabuck, K. Raghavachari, J.B. Foresman, J.V. Ortiz, Q. Cui, A.G. Baboul, S. Clifford, J. Cioslowski, B.B. Stefanov, G. Liu, A. Liashenko, P. Piskorz, I. Komaromi, R.L. Martin, D.J. Fox, T. Keith, M.A. Al-Laham, C.Y. Peng, A. Nanayakkara, M. Challacombe, P.M.W. Gill, B. Johnson, W. Chen, M.W. Wong, C. Gonzalez, J.A. Pople, *Gaussian 03: Computer Program for Computational Chemistry* (Gaussian Inc., Pittsburgh, 2004)
31. M. Amirnasr, M. Bagheri, H. Farrokhpour, K.J. Schenk, K. Mereiter, P.C. Ford, Polyhedron **29**, 71 (2014)
32. B. Mishra, B.B. Patel, S. Tiwari, Nanomedicine **6**, 1 (2010)
33. A. Zebardasti, A. Kakanejadifard, L. Shabani, Bull. Chem. Soc. Ethiop. **26**, 1 (2012)
34. A.B. Gündüzalp, İ. Özsen, H. Alyar, S. Alyar, N. Özbek, J. Mol. Struct. **15**, 1120 (2016)
35. A. El-Sonbati, M. Diab, A. El-Bindary, M. Abou-Dobara, H. Seyam, J. Mol. Liq. **1**, 218 (2016)
36. I. Wakil, N. Ndahi, M. Abubakar, I. Waziri, Chem. Res. J. **2**, 2 (2017)
37. D.M.A. El-Aziz, S.E.H. Etaiw, E.A. Ali, J. Mol. Strut. **24**, 1048 (2013)
38. T.C. Zeyrek, J. Korean Chem. Soc. **57**, 4 (2013)
39. P. Wayne, CLSI document M27-A2 (2002)
40. J. Feng, K. Ablajan, A. Sali, Tetrahedron **70**, 2 (2014)
41. B.M. Rao, G.N. Reddy, T.V. Reddy, B.P. Devi, R. Prasad, J. Yadav, B.S. Reddy, Tetrahedron Lett. **54**, 20 (2013)
42. D. Van Der Spoel, E. Lindahl, B. Hess, G. Groenhof, A.E. Mark, H.J. Berendsen, J. Comput. Chem. **26**, 16 (2005)
43. G.M. Morris, R. Huey, W. Lindstrom, M.F. Sanner, R.K. Belew, D.S. Goodsell, A.J. Olson, J. Comput. Chem. **30**, 16 (2009)
44. W. Humphrey, A. Dalke, K. Schulten, J. Mol. Graph. **14**, 1 (1996)

Affiliations

Elham Zarenezhad[1] · Sheida Esmaielzadeh[2] · Somayeh Behrouz[3] · Leila Emami[4]

[1] Noncommunicable Diseases Research Center, Fasa University of Medical Sciences, Fasa, Iran

[2] Department of Chemistry, Darab Branch, Islamic Azad University, Darab, Islamic Republic of Iran

[3] Medicinal Chemistry Research Laboratory, Department of Chemistry, Shiraz University of Technology, Shiraz 71555-313, Iran

[4] Faculty of Pharmacy, Shiraz University of Medical Sciences, Shiraz, Islamic Republic of Iran